Hindawi
Advances in Civil Engineering
Volume 2018, Article ID 3854620, 16 pages
https://doi.org/10.1155/2018/3854620

Research Article

Optimum Design of Braced Steel Space Frames including Soil-Structure Interaction via Teaching-Learning-Based Optimization and Harmony Search Algorithms

Ayse T. Daloglu,[1] **Musa Artar**,[2] **Korhan Ozgan**,[1] **and Ali İ. Karakas**[1]

[1]*Department of Civil Engineering, Karadeniz Technical University, Trabzon, Turkey*
[2]*Department of Civil Engineering, Bayburt University, Bayburt, Turkey*

Correspondence should be addressed to Korhan Ozgan; korhanozgan@yahoo.com

Received 19 August 2017; Revised 13 November 2017; Accepted 6 December 2017; Published 3 April 2018

Academic Editor: Moacir Kripka

Optimum design of braced steel space frames including soil-structure interaction is studied by using harmony search (HS) and teaching-learning-based optimization (TLBO) algorithms. A three-parameter elastic foundation model is used to incorporate the soil-structure interaction effect. A 10-storey braced steel space frame example taken from literature is investigated according to four different bracing types for the cases with/without soil-structure interaction. X, V, Z, and eccentric V-shaped bracing types are considered in the study. Optimum solutions of examples are carried out by a computer program coded in MATLAB interacting with SAP2000-OAPI for two-way data exchange. The stress constraints according to AISC-ASD (American Institute of Steel Construction-Allowable Stress Design), maximum lateral displacement constraints, interstorey drift constraints, and beam-to-column connection constraints are taken into consideration in the optimum design process. The parameters of the foundation model are calculated depending on soil surface displacements by using an iterative approach. The results obtained in the study show that bracing types and soil-structure interaction play very important roles in the optimum design of steel space frames. Finally, the techniques used in the optimum design seem to be quite suitable for practical applications.

1. Introduction

Optimum design of steel structures prevents excessive consumption of the steel material. Suitable cross sections must be selected automatically from a predefined list. Moreover, selected profiles should satisfy some required constraints such as stress, displacement, and geometric size. Metaheuristic search techniques are highly preferred for problems with discrete design variables. There are many metaheuristic techniques developed recently. Some of them are genetic algorithm, harmony search algorithm, tabu search algorithm, particle swarm optimization, ant colony algorithm, artificial bee colony algorithm, teaching-learning-based optimization, simulated annealing algorithm, bat-inspired algorithm, cuckoo search algorithm, and evolutionary structural optimization. In literature, there are many studies available for the optimum design of structures using these algorithms. For example, Daloglu and Armutcu [1] used the genetic algorithm method for the optimum design of plane steel frames. Kameshki and Saka [2] carried out the optimum design of nonlinear steel frames with semirigid connections using the genetic algorithm. Lee and Geem [3] developed a new structural optimization method based on the harmony search algorithm. Hayalioglu and Degertekin [4] applied genetic optimization on minimum cost design of steel frames with semirigid connections and column bases. Kelesoglu and Ülker [5] searched for multiobjective fuzzy optimization of space trusses by MS Excel. Degertekin [6] compared simulated annealing and genetic algorithms for the optimum design of nonlinear steel space frames. Esen and Ülker [7] optimized multistorey space steel frames considering the nonlinear material and geometrical properties. Saka [8] used the harmony search algorithm method to get the optimum design of steel sway frames

in accordance with BS5950. Degertekin and Hayalioglu [9] applied the harmony search algorithm for minimum cost design of steel frames with semirigid connections and column bases. Hasancebi et al. [10] investigated nondeterministic search techniques in the optimum design of real-size steel frames. Hasançebi et al. [11] used the simulated annealing algorithm in structural optimization. Hasancebi et al. [12] investigated the optimum design of high-rise steel buildings using an evolutionary strategy integrated with parallel algorithm. Togan [13] used one of the latest stochastic methods, teaching-learning-based optimization, for design of planar steel frames. Aydogdu and Saka [14] used ant colony optimization for irregular steel frames including the elemental warping effect. Dede and Ayvaz [15] studied structural optimization problems using the teaching-learning-based optimization algorithm. Dede [16] applied teaching-learning-based optimization on the optimum design of grillage structures with respect to LRFD-AISC. Hasançebi et al. [17] used a bat-inspired algorithm for structural optimization. Saka and Geem [18] prepared an extensive review study on mathematical and metaheuristic applications in design optimization of steel frame structures. Hasançebi and Çarbaş [19] studied the bat-inspired algorithm for discrete-size optimization of steel frames. Dede [20] focused on the application of the teaching-learning-based optimization algorithm for the discrete optimization of truss structures. Azad and Hasancebi [21] focused on discrete-size optimization of steel trusses under multiple displacement constraints and load case using the guided stochastic search technique. Artar and Daloğlu [22] obtained the optimum design of composite steel frames with semirigid connections and column bases. Artar [23] used the harmony search algorithm for the optimum design of steel space frames under earthquake loading. Artar [24] used the teaching-learning-based optimization algorithm for the optimum design of braced steel frames. Carbas [25] studied design optimization of steel frames using an enhanced firefly algorithm. Daloglu et al. [26] investigated the optimum design of steel space frames including soil-structure interaction. Saka et al. [27] researched metaheuristics in structural optimization and discussions on the harmony search algorithm. Aydogdu [28] used a biogeography-based optimization algorithm with Levy flights for cost optimization of reinforced concrete cantilever retaining walls under seismic loading.

In literature, there are several researches available for optimum structural design, as mentioned above. On the other hand, there are a few researches on the optimum design of braced steel space frames including soil-structure interaction. So, this study investigates a 10-storey braced steel space frame structure studied previously in literature, which is investigated for four different bracing types and soil-structure interaction. These bracing types are X, V, Z, and eccentric V-shaped bracings. Optimum design solutions are obtained using a computer program developed in MATLAB [29] interacting with SAP2000-OAPI (open application programming interface) [30]. Suitable cross sections are automatically selected from a list including 128 W profiles taken from AISC (American Institute of Steel Construction). The frame model is subjected to wind loads according to ASCE7-05 [31] as well as dead, live, and snow loads. The analysis results are found to be quite consistent with the literature results. In this study, the vertical displacements on soil surfaces are also calculated. It is observed that minimum weights of space frames vary depending on the bracing type. Also, it can be concluded that incorporation of soil-structure interaction results in heavier steel weight.

2. Optimum Design Formulation

The optimum design problem of braced steel space frames is calculated as follows:

$$\min W = \sum_{k=1}^{\mathrm{ng}} A_k \sum_{i=1}^{\mathrm{nk}} \rho_i L_i, \tag{1}$$

where W is the weight of the frame, A_k is the cross-sectional area of group k, ρ_i and L_i are the density and length of member i, ng is the total number of groups, and nk is the total number of members in group k.

The stress constraints according to AISC-ASD [32] are defined as follows:

$$g_i(x) = \left[\frac{f_{\mathrm{a}}}{F_{\mathrm{a}}} + \frac{C_{\mathrm{m}x} f_{\mathrm{b}x}}{\left(1 - \left(f_{\mathrm{a}}/F'_{\mathrm{e}x}\right)\right) F_{\mathrm{b}x}}\right]_i - 1.0 \le 0, \quad i = 1, \ldots, \mathrm{nc},$$

$$g_i(x) = \left[\frac{f_{\mathrm{a}}}{0.60 F_{\mathrm{y}}} + \frac{f_{\mathrm{b}x}}{F_{\mathrm{b}x}}\right]_i - 1.0 \le 0, \quad i = 1, \ldots, \mathrm{nc}. \tag{2}$$

If $(f_{\mathrm{a}}/F_{\mathrm{a}}) \le 0.15$, instead of using (2), the stress constraint is calculated as follows:

$$g_i(x) = \left[\frac{f_{\mathrm{a}}}{F_{\mathrm{a}}} + \frac{f_{\mathrm{b}x}}{F_{\mathrm{b}x}}\right]_i - 1.0 \le 0, \quad i = 1, \ldots, \mathrm{nc}, \tag{3}$$

where nc is the total number of members subjected to both axial compression and bending stresses, f_{a} is the computed axial stress, F_{a} is the allowable axial stress under axial compression force alone, $f_{\mathrm{b}x}$ is the computed bending stress due to bending of the member about its major (x), $F_{\mathrm{b}x}$ is the allowable compressive bending stress about major, F'_{ex} is the Euler stress, F_{y} is the yield stress of the steel, and $C_{\mathrm{m}x}$ is a factor. It is calculated from $C_{\mathrm{m}x} = 0.6 - 0.4(M1/M2)$ for the braced frame member without transverse loading between the ends and $C_{\mathrm{m}x} = 1 + \psi(f_{\mathrm{a}}/F'_{\mathrm{e}})$ for the braced frame member with transverse loading.

The effective length factors of columns in braced frames are calculated as follows [33]:

$$K = \frac{3G_{\mathrm{A}}G_{\mathrm{B}} + 1.4\left(G_{\mathrm{A}} + G_{\mathrm{B}}\right) + 0.64}{3G_{\mathrm{A}}G_{\mathrm{B}} + 2.0\left(G_{\mathrm{A}} + G_{\mathrm{B}}\right) + 1.28}, \tag{4}$$

where G_{A} and G_{B} are the relative stiffness factors at the Ath and Bth ends of columns.

The maximum lateral displacement and interstorey drift constraints are defined as follows:

$$g_{jl}(x) = \frac{\delta_{jl}}{\delta_{ju}} - 1 \le 0, \quad j = 1, \ldots, m, \quad l = 1, \ldots, \text{nl}, \tag{5}$$

where δ_{jl} is the displacement of the jth degree of freedom under load case l, δ_{ju} is the displacement at the upper bound, m is the number of restricted displacements, and nl is the total number of loading cases.

$$g_{jil}(x) = \frac{\Delta_{jil}}{\Delta_{ju}} - 1 \le 0, \quad j = 1, \ldots, \text{ns}, \quad i = 1, \ldots, \text{nsc}, \quad l = 1, \ldots, \text{nl}, \tag{6}$$

where Δ_{jil} is the interstorey drift of the ith column in the jth storey under load case l, Δ_{ju} is the limit value, ns is the number of storeys, and nsc is the number of columns in a storey.

The beam-to-column connection geometric constraint is determined as follows:

$$g_{\text{bf},i}(x) = \frac{b'_{\text{fb}k,i}}{d_{\text{c},i} - 2t_{\text{fl},i}} - 1 \le 0, \quad i = 1, \ldots, n_{\text{bw}}, \qquad g_{\text{bb},i}(x) = \frac{b_{\text{fb}k,i}}{b_{\text{fc}k,i}} - 1 \le 0, \quad i = 1, \ldots, n_{\text{bf}}, \tag{7}$$

where n_{bw} is the number of joints where beams are connected to the web of the column, $b'_{\text{fb}k,i}$ is the flange width of the beam, $d_{\text{c},i}$ is the depth of the column, $t_{\text{fl},i}$ is the flange thickness of the column, n_{bf} is the number of joints where beams are connected to the flange of the column, and $b_{\text{fb}k,i}$ and $b_{\text{fc}k,i}$ are flange widths of the beam and column, respectively (Figure 1).

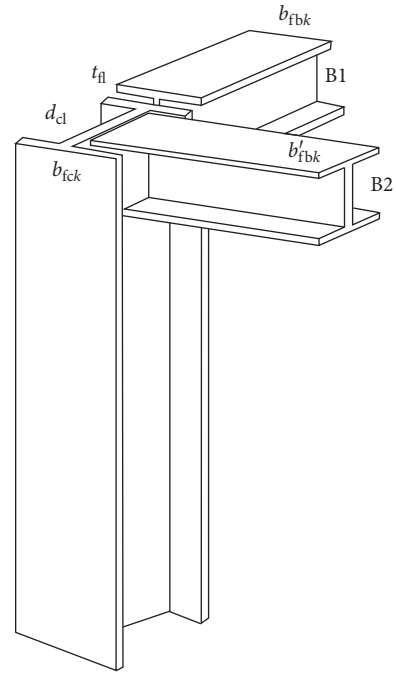

Figure 1: Beam-to-column connection geometric constraints.

3. Three-Parameter Vlasov Elastic Foundation Model

The soil reaction exerted on a structure resting on a two-parameter elastic soil is expressed in

$$q_z = kw - 2t\nabla^2 w. \tag{8}$$

The reaction depends on the soil surface vertical displacement w, soil reaction modulus k, and soil shear parameter $2t$. These two soil parameters, k and $2t$, can be defined by

$$k = \int_0^H \frac{E_{\text{s}}(1-v_{\text{s}})}{(1+v_{\text{s}})(1-2v_{\text{s}})} \cdot \left(\frac{\partial \varphi(z)}{\partial z}\right)^2 dz, \qquad 2t = \int_0^H G_{\text{s}} \varphi(z)^2 \, dz, \tag{9}$$

in which H, v_{s}, and G_{s} are the depth, Poisson's ratio, and shear modulus of the soil, respectively. In most of the classical two-parameter soil foundation models such as Pasternak, Hetenyi, and Vlasov models, the soil parameters are constants obtained by experimental tests or arbitrarily defined. However, it is highly difficult to determine these parameters experimentally. Therefore, Vallabhan and Daloglu [34] developed an additional parameter γ to characterize the vertical displacement profile within subsoil. They called this model including the third parameter γ as a three-parameter Vlasov model. This model eliminates the necessity of experimental tests to determine soil parameters since these values are determined iteratively in terms of the new parameter, γ. The vertical deformation profile of the subsoil is described via a mode shape function as given in

$$\phi(z) = \frac{\sinh \gamma (1 - (z/H))}{\sinh \gamma}. \tag{10}$$

The boundary values of $\phi(z)$ are assumed to be $\phi(0) = 1$ and $\phi(H) = 0$, as shown in Figure 2. The γ parameter can be calculated using

$$\left(\frac{\gamma}{H}\right)^2 = \frac{(1-2\nu_s)}{2(1-\nu_s)} \cdot \frac{\int_{-\infty}^{+\infty}\int_{-\infty}^{+\infty} (\nabla w)^2 \, dx \, dy}{\int_{-\infty}^{+\infty}\int_{-\infty}^{+\infty} w^2 \, dx \, dy}. \tag{11}$$

Equation (9) indicates that the soil parameters (k and $2t$) are calculated based on the material properties and mode shape function ($\varphi(z)$). Also, it is necessary to compute the γ parameter to calculate the mode shape function. It is necessary to know the soil vertical surface displacements obtained from the structural analysis to calculate the γ parameter. So, it can be stated that k, $2t$, ϕ, γ, and w are interdependent. That is why the analysis requires an iterative procedure. For this purpose, a computer program is coded in MATLAB interacting with SAP2000 structural analysis program via OAPI (open application programming interface) to perform this iterative procedure in the three-parameter foundation model.

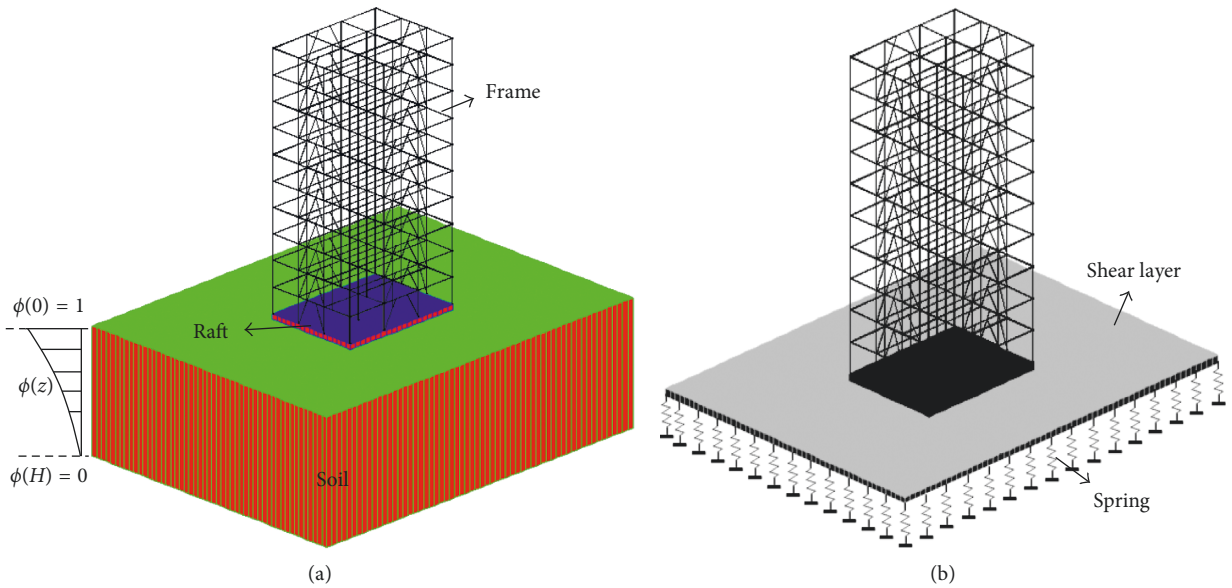

Figure 2: A space frame on three-parameter elastic foundation. (a) 3D frame on elastic subsoil. (b) Mathematical model.

Using the coded program, a soil model is generated such that the soil reaction modulus k is represented by elastic area springs. The interaction between springs is taken into account using shell elements connecting the top of springs. The soil shell element with one degree of freedom at each node reflects only shear behavior of the soil. The γ parameter is computed numerically in the coded program using the vertical displacements of soil shell elements. To determine the soil parameters iteratively, $\gamma = 1$ is assumed initially and k and $2t$ values are calculated. Then, the structural model is analyzed using SAP2000, and the soil surface vertical displacements are retrieved to compute a new γ value. The difference between successive values of γ is calculated and checked whether it is within a prescribed tolerance or not. If it is smaller than the tolerance, the iteration is terminated. Otherwise, the next iteration is performed, and the procedure is repeated until the convergence is fulfilled.

4. Optimization Algorithms

4.1. Harmony Search Algorithm. Harmony search (HS) algorithm method is developed by Lee and Geem [3] and mimics improvisation procedures of musical harmony. It consists of three basic procedures. Operations are conducted by the harmony memory (HM) matrix. In the first step, HM is randomly and automatically filled by the program coded in MATLAB. The form of harmony memory matrix is shown as follows:

$$H = \begin{bmatrix} x_1^1 & x_2^1 & \cdots & x_{n-1}^1 & x_n^1 \\ x_1^2 & x_2^2 & \cdots & x_{n-1}^2 & x_n^2 \\ \vdots & \vdots & \vdots & \vdots & \vdots \\ x_1^{\mathrm{HMS}-1} & x_2^{\mathrm{HMS}-1} & \cdots & x_{n-1}^{\mathrm{HMS}-1} & x_n^{\mathrm{HMS}-1} \\ x_1^{\mathrm{HMS}} & x_2^{\mathrm{HMS}} & \cdots & x_{n-1}^{\mathrm{HMS}} & x_n^{\mathrm{HMS}} \end{bmatrix} \begin{matrix} \rightarrow \\ \rightarrow \\ \rightarrow \\ \rightarrow \\ \rightarrow \end{matrix} \begin{matrix} \varphi(x^1) \\ \varphi(x^2) \\ \vdots \\ \varphi(x^{\mathrm{HMS}-1}) \\ \varphi(x^{\mathrm{HMS}}) \end{matrix}, \tag{12}$$

where x_i^j is the ith design variable of the jth solution vector, n is the total number of design variables, $\varphi(x^j)$ is the jth objective function value, and HMS (harmony memory size) indicates a specified number of solutions. In the harmony memory matrix, each row presents design variables.

In the second step, the objective function values $(\varphi(x^1), \varphi(x^2) \cdots \varphi(x^{\mathrm{HMS}-1}), \varphi(x^{\mathrm{HMS}}))$ of solution vectors in the harmony memory matrix are determined. In the third step, a new solution vector $(x^{\mathrm{nh}} = [x_1^{\mathrm{nh}}, x_2^{\mathrm{nh}}, \ldots, x_n^{\mathrm{nh}}])$ is prepared by selecting each design variable from either the harmony memory matrix or the entire section list X_{sl}. Harmony memory consideration rate (HMCR) is applied as follows:

$$\begin{aligned} &x_i^{\mathrm{nh}} \in \{x_i^1, x_i^2, \ldots, x_i^{\mathrm{HMS}}\} \text{ with probability of HMCR} \\ &x_i^{\mathrm{nh}} \in X_{\mathrm{sl}} \text{ with probability of } (1 - \mathrm{HMCR}). \end{aligned} \tag{13}$$

Also, the new value of the design variable selected from the harmony memory matrix is checked whether this value should be pitch adjusted or not depending on the pitch adjustment ratio (PAR). This decision is determined as follows:

$$\begin{aligned} &\text{Yes, with probability of PAR} \\ &\text{No, with probability of } 1 - \mathrm{PAR}. \end{aligned} \tag{14}$$

Detailed information about the HS algorithm can be found in the literature [3, 8, 9, 23].

4.2. Teaching-Learning-Based Optimization. Teaching-learning-based optimization (TLBO) was developed by Rao et al. [35]. This method mimics teaching and learning processes between a teacher and students in classroom. The person having the highest information in the class is selected as a teacher. The teacher gives his/her information to the other

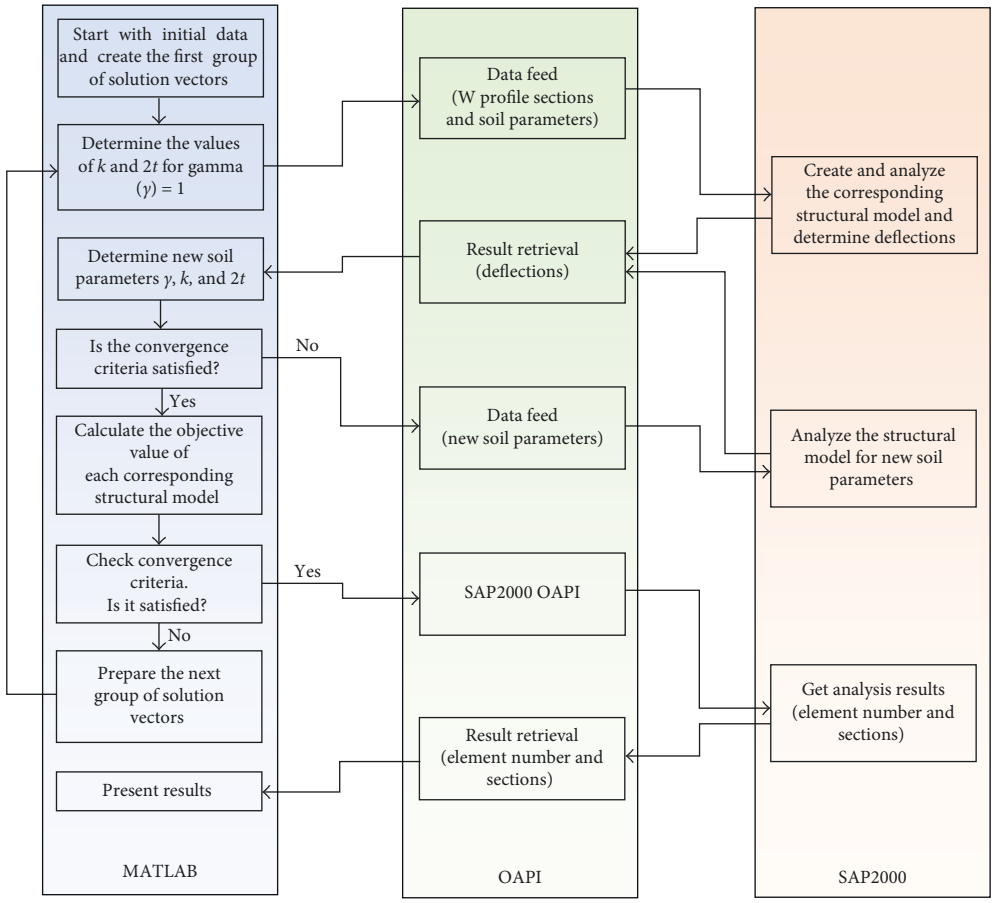

Figure 3: Flowchart for the optimum design algorithm by HS and TLBO for space frames on elastic foundation.

people (students) in the class. These procedures provide suitable solutions in structural optimizations. The teaching-learning-based optimization method consists of two basic steps such as teaching and learning. In the first step, the teaching step, the first population (class) is randomly filled in the matrix form presented as follows:

$$\text{class}(\text{population}) = \begin{bmatrix} x_1^1 & x_2^1 & \cdots & x_{n-1}^1 & x_n^1 \\ x_1^2 & x_2^2 & \cdots & x_{n-1}^2 & x_n^2 \\ \vdots & \vdots & \vdots & \vdots & \vdots \\ x_1^{S-1} & x_2^{S-1} & \cdots & x_{n-1}^{S-1} & x_n^{S-1} \\ x_1^S & x_2^S & \cdots & x_{n-1}^S & x_n^S \end{bmatrix} \begin{matrix} \rightarrow & f(x^1) \\ \rightarrow & f(x^2) \\ \rightarrow & \vdots \\ \rightarrow & f(x^{S-1}) \\ \rightarrow & f(x^S) \end{matrix}, \tag{15}$$

where each row represents a student and gives a design solution, S is the population size (the number of students), n is the number of design variables, and $f(x^{1,2,\ldots,S})$ is the unconstrained objective function value of each student in the class. The student in a class having the best information is selected as a teacher of the class. His or her objective function value is the minimum in the class. The information update of students in the class is carried out with the help of the teacher as follows:

$$x^{\text{new},i} = x^i + r\left(x_{\text{teacher}} - T_F x_{\text{mean}}\right), \tag{16}$$

where $x^{\text{new},i}$ is the new student, x^i is the current student, r is a random number in the range [0,1], and T_F, a teaching factor, is either 1 or 2. x_{mean} is the mean of the class defined as $x_{\text{mean}} = (\text{mean}(x_1)....\text{mean}(x_S))$. If the new student has better information $(f(x^{\text{new},i}))$, the new student is replaced with the current student. In the second step, the learning step, information is shared between students. This step is similar to the first step. If the new student presents a better information, he/she is replaced with the current student. The information update of students in the class is carried out as follows:

$$\begin{aligned} &\text{if } f(x^i) < f(x^j) \Rightarrow x^{\text{new},i} = x^i + r\left(x^i - x^j\right), \\ &\text{if } f(x^i) > f(x^j) \Rightarrow x^{\text{new},i} = x^i + r\left(x^j - x^i\right). \end{aligned} \tag{17}$$

The detailed information about the TLBO algorithm can be obtained from [13, 15, 16, 20, 24, 35]. The flowchart of processes in MATLAB-SAP2000 OAPI developed to get optimum solutions is presented in Figure 3.

5. Design Example

A 10-storey braced steel space frame example taken from literature [36] is studied considering four different types of

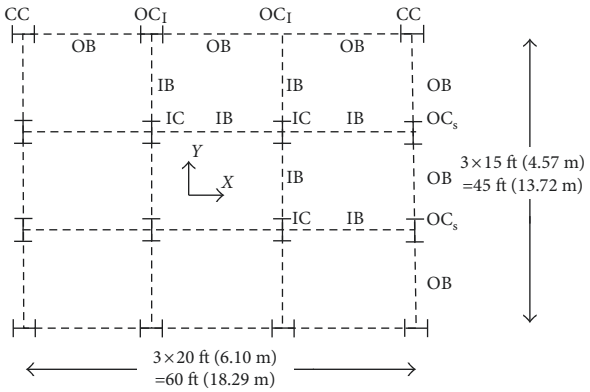

Figure 4: Typical plane view of a 10-storey steel frame.

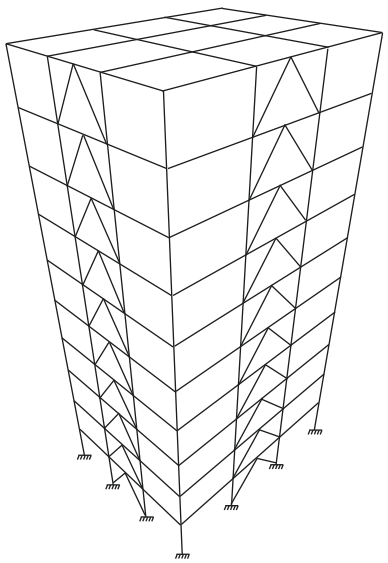

Figure 5: Three dimensional view of a V-braced frame.

Table 1: Gravity loading on beams of roof and floors [36].

Beam type	Outer span beams (kN/m)	Inner span beams (kN/m)
Long span floor beams	9.79	19.59
Short span floor beams	8.04	16.07
Long span roof beams	6.75	13.50
Short span floor beams	5.54	11.07

bracing such as X, V, Z, and eccentric V. The behavior of the frame is investigated with and without considering the effect of soil-structure interaction. The frame example is exposed to wind loads according to ASCE7-05 [31] in addition to dead, live, and snow loads. Optimum cross sections are practically selected from a predefined list of 128 W profiles taken from AISC. The stress constraints according to AISC-ASD [32], maximum lateral displacement constraint (H/400), interstorey drift constraint (h/400), and beam-to-column geometric constraints are subjected to the optimum design of the braced steel space frames. In the analyses, the steel modulus of elasticity, E, and yield stress, F_y, are taken as

Table 2: Wind loads calculated for the 10-storey braced frame [36].

Floor	X-direction		Y-direction	
	Distributed windward force (kN/m)	Distributed leeward force (kN/m)	Distributed windward force (kN/m)	Distributed leeward force (kN/m)
1	2.33	2.32	2.33	2.63
2	2.66	2.32	2.66	2.63
3	2.99	2.32	2.99	2.63
4	3.24	2.32	3.24	2.63
5	3.46	2.32	3.46	2.63
6	3.64	2.32	3.64	2.63
7	3.81	2.32	3.81	2.63
8	3.95	2.32	3.95	2.63
9	4.09	2.32	4.09	2.63
10	2.11	1.16	2.11	1.32

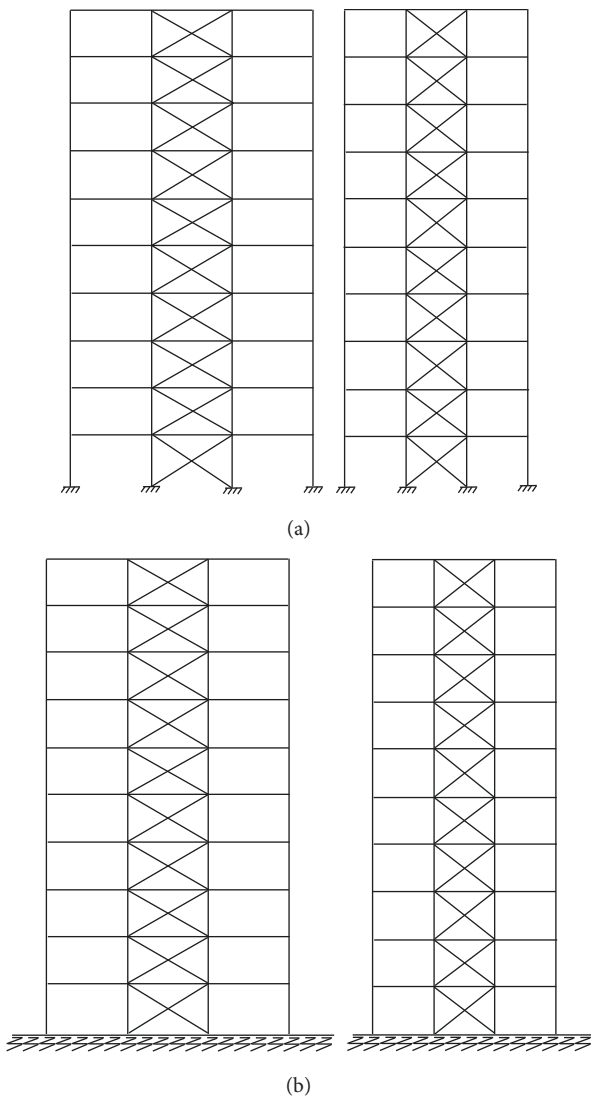

(a)

(b)

Figure 6: 2D view of the X-braced steel space frame without and with soil-structure interaction. (a) The case without soil-structure interaction. (b) The case with soil-structure interaction.

Table 3: Optimum results of the X-braced space frame.

Storeys	Member groups	Literature research, Hasancebi [36]	This study			
			TLBO without soil-structure interaction	TLBO with soil-structure interaction	HS without soil-structure interaction	HS with soil-structure interaction
	CC	W16 × 36	W8 × 24	W8 × 28	W8 × 35	W8 × 31
	OC_l	W12 × 65	W21 × 83	W14 × 99	W14 × 43	W12 × 50
	OC_s	W24 × 94	W44 × 224	W44 × 224	W12 × 50	W18 × 50
1-2	IC	W12 × 120	W14 × 74	W16 × 89	W18 × 97	W18 × 119
	OB	W8 × 18	W8 × 24	W10 × 26	W8 × 24	W8 × 24
	IB	W18 × 35	W10 × 33	W14 × 48	W10 × 33	W16 × 40
	BR	W5 × 19	W8 × 15	W12 × 16	W8 × 21	W8 × 15
	CC	W10 × 33	W8 × 28	W8 × 28	W14 × 48	W10 × 60
	OC_l	W10 × 54	W12 × 87	W10 × 49	W10 × 33	W12 × 65
	OC_s	W12 × 72	W10 × 49	W12 × 53	W24 × 68	W24 × 76
3-4	IC	W30 × 90	W24 × 62	W12 × 72	W14 × 68	W24 × 94
	OB	W8 × 18	W12 × 30	W8 × 24	W18 × 50	W18 × 50
	IB	W12 × 26	W14 × 34	W8 × 35	W10 × 33	W12 × 35
	BR	W6 × 15	W12 × 14	W12 × 14	W10 × 15	W6 × 15
	CC	W16 × 31	W16 × 36	W8 × 31	W14 × 34	W14 × 43
	OC_l	W10 × 49	W8 × 35	W14 × 34	W8 × 28	W12 × 45
	OC_s	W10 × 54	W8 × 40	W10 × 60	W14 × 38	W16 × 50
5-6	IC	W12 × 58	W24 × 55	W14 × 53	W16 × 57	W18 × 65
	OB	W8 × 21	W16 × 36	W10 × 30	W10 × 30	W10 × 30
	IB	W12 × 26	W16 × 36	W14 × 38	W16 × 45	W18 × 50
	BR	W6 × 15	W10 × 15	W12 × 14	W12 × 22	W6 × 15
	CC	W16 × 26	W8 × 24	W12 × 53	W10 × 45	W10 × 45
	OC_l	W10 × 49	W8 × 31	W10 × 49	W12 × 45	W12 × 45
	OC_s	W10 × 49	W10 × 54	W12 × 53	W10 × 45	W14 × 48
7-8	IC	W14 × 38	W16 × 36	W14 × 43	W14 × 48	W10 × 68
	OB	W8 × 21	W8 × 24	W10 × 30	W8 × 35	W12 × 35
	IB	W12 × 26	W14 × 34	W18 × 40	W10 × 33	W10 × 33
	BR	W6 × 9	W12 × 14	W12 × 14	W12 × 14	W12 × 14
	CC	W12 × 26	W8 × 28	W8 × 24	W8 × 31	W12 × 40
	OC_l	W8 × 31	W10 × 49	W14 × 30	W10 × 33	W14 × 53
	OC_s	W8 × 40	W8 × 31	W12 × 40	W14 × 30	W14 × 30
9-10	IC	W8 × 28	W12 × 30	W12 × 40	W16 × 36	W12 × 45
	OB	W8 × 18	W8 × 24	W8 × 24	W21 × 44	W8 × 24
	IB	W12 × 30	W21 × 44	W10 × 33	W16 × 36	W10 × 39
	BR	W6 × 9	W10 × 15	W10 × 15	W12 × 14	W12 × 14
Weight (kN)		1092.91	1170.03	1217.91	1201.13	1265.50
Maximum lateral displacement (cm)		—	6.36	7.59	7.92	8.29
Interstorey drift (cm)		—	0.81	0.91	0.915	0.915
Maximum settlement (cm)		—	—	−0.657	—	−0.670

29000 ksi (203,893.6 MPa) and 36 ksi (253.1 MPa), respectively. Figure 4 shows the typical plane view of a 10-storey steel frame. Also, Figure 5 represents the three dimensional view of a V-braced frame. Each storey has a height of 3.66 m (12 ft). Modulus of elasticity for the concrete is taken as 32,000,000 kN/m^2, Poisson's ratio is 0.2, and weight per unit volume is 25 kN/m^3.

All floors excluding the roof are exposed to a dead load of 2.88 kN/m^2 and a live load of 2.39 kN/m^2. The roof floor is exposed to a dead load of 2.88 kN/m^2 and a snow load of 0.75 kN/m^2. The total gravity loading on the beams of roof and floors is tabulated in Table 1 [36]. Wind loads are applied to the frame according to ASCE7-05 [31]. Wind loads calculated for the 10-storey braced frame are presented in Table 2 [36]. Modulus of elasticity of the soil, E_s, is taken to be equal to 80,000 kN/m^2. The depth of the soil stratum to the rigid base is taken as $H_s = 20$ m, and Poisson's ratio of the soil is equal to 0.25.

Table 4: Soil parameters for 10-storey X-braced steel space frame on elastic foundation.

Algorithm	γ	k (kN/m^3)	$2t$ (kN/m^3)
Teaching-learning-based optimization	4.52365	10882.438	70605.337
Harmony search algorithm	4.51999	10873.807	70661.621

5.1. X-Braced Steel Space Frame. Figure 6 shows the typical 2D view of an X-braced steel space frame without and with soil-structure interaction. Optimum results of the X-braced space frame are given in Table 3. Soil parameters for the

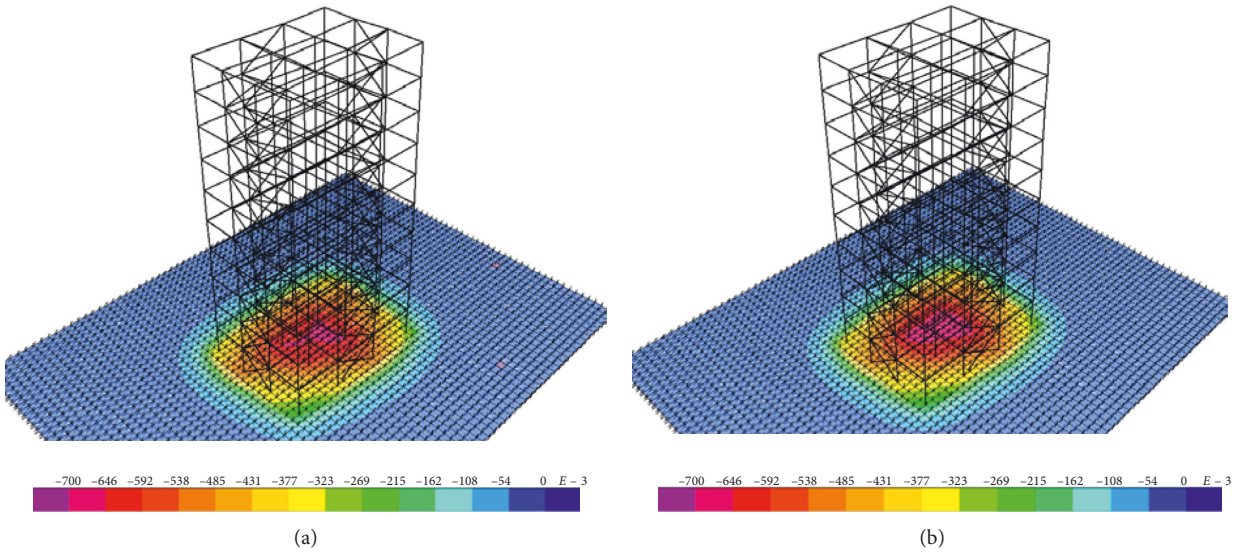

Figure 7: Settlements of soil surface for the X-braced steel space frame with two different algorithm methods (cm). (a) TLBO. (b) HS.

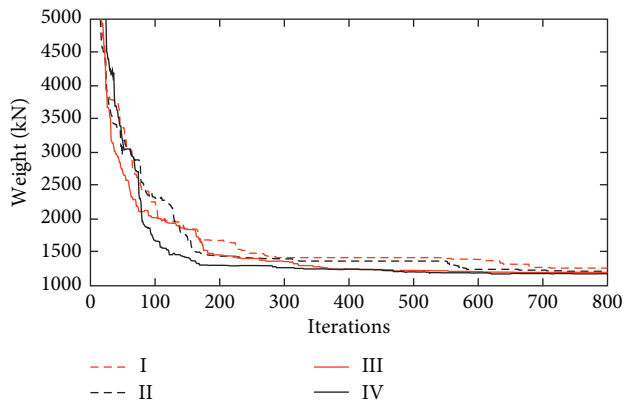

Figure 8: Design histories of the 10-storey X-braced steel space frame. I: HS with soil-structure interaction; II: TLBO with soil-structure interaction; III: HS without soil-structure interaction; IV: TLBO without soil-structure interaction.

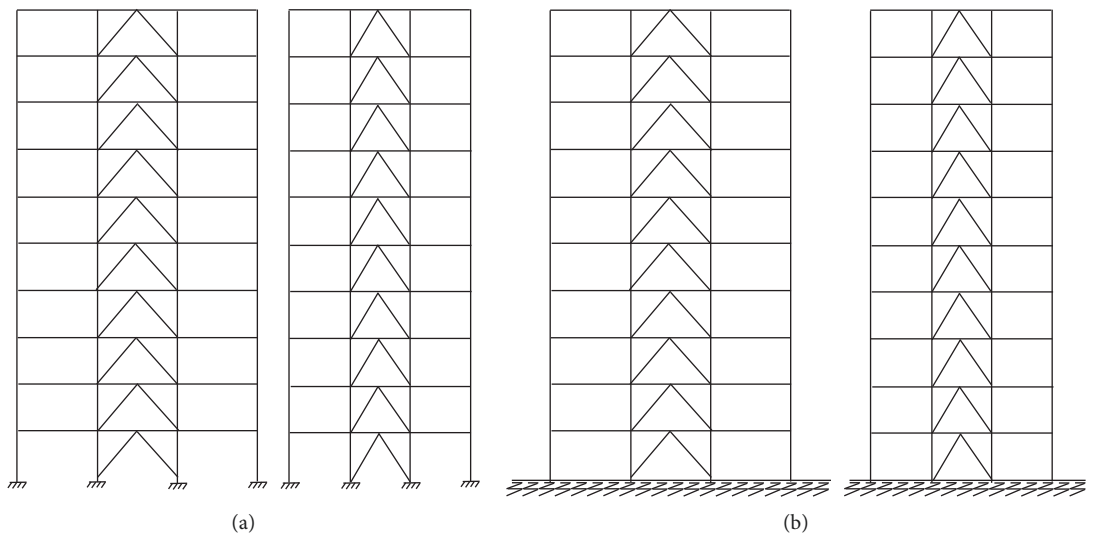

Figure 9: 2D view of the V-braced steel space frame without and with soil-structure interaction. (a) The case without soil-structure interaction. (b) The case with soil-structure interaction.

Table 5: Optimum results of the V-braced space frame.

Storeys	Member groups	Literature research, Hasancebi [36]	This study			
			TLBO without soil-structure interaction	TLBO with soil-structure interaction	HS without soil-structure interaction	HS with soil-structure interaction
	CC		W8 × 28	W8 × 31	W8 × 28	W8 × 28
	OC_l		W14 × 43	W16 × 67	W16 × 50	W12 × 50
	OC_s		W44 × 224	W27 × 161	W16 × 67	W18 × 106
1-2	IC		W10 × 88	W18 × 106	W18 × 106	W14 × 132
	OB		W8 × 28	W14 × 34	W8 × 24	W8 × 24
	IB		W10 × 33	W10 × 33	W8 × 35	W10 × 33
	BR		W12 × 14	W6 × 15	W8 × 21	W12 × 14
	CC		W8 × 24	W8 × 24	W8 × 31	W8 × 24
	OC_l		W12 × 45	W10 × 49	W12 × 35	W21 × 44
	OC_s		W10 × 45	W18 × 86	W10 × 45	W16 × 40
3-4	IC		W21 × 62	W21 × 68	W14 × 68	W18 × 65
	OB		W8 × 24	W10 × 30	W8 × 24	W8 × 24
	IB		W12 × 35	W8 × 35	W12 × 35	W16 × 40
	BR		W5 × 16	W8 × 21	W14 × 22	W10 × 26
	CC		W12 × 30	W8 × 24	W10 × 39	W10 × 33
	OC_l		W14 × 34	W8 × 31	W16 × 36	W16 × 36
	OC_s		W18 × 46	W14 × 48	W18 × 55	W18 × 50
5-6	IC		W12 × 50	W18 × 55	W24 × 55	W21 × 62
	OB		W10 × 30	W8 × 24	W14 × 38	W14 × 38
	IB		W8 × 35	W16 × 36	W14 × 38	W18 × 50
	BR		W10 × 15	W12 × 19	W12 × 22	W6 × 15
	CC		W8 × 28	W8 × 24	W14 × 53	W16 × 77
	OC_l		W8 × 28	W8 × 35	W12 × 45	W8 × 35
	OC_s		W8 × 24	W12 × 30	W10 × 45	W8 × 35
7-8	IC		W16 × 40	W16 × 45	W10 × 39	W12 × 40
	OB		W10 × 30	W8 × 24	W8 × 31	W8 × 35
	IB		W16 × 36	W14 × 34	W10 × 33	W18 × 40
	BR		W12 × 14	W12 × 16	W8 × 21	W12 × 22
	CC		W12 × 30	W8 × 28	W14 × 48	W12 × 40
	OC_l		W10 × 33	W8 × 24	W8 × 35	W8 × 40
	OC_s		W8 × 31	W8 × 24	W8 × 35	W8 × 35
9-10	IC		W24 × 55	W12 × 26	W16 × 36	W16 × 36
	OB		W8 × 24	W8 × 24	W8 × 31	W8 × 31
	IB		W16 × 36	W18 × 40	W14 × 34	W16 × 36
	BR		W10 × 15	W10 × 15	W12 × 14	W12 × 14
Weight (kN)		1082.80	1083.80	1101.27	1118.04	1185.53
Maximum lateral displacement (cm)		—	6.93	7.91	8.01	7.99
Interstorey drift (cm)		—	0.91	0.91	0.915	0.91
Maximum settlement (cm)		—	—	−0.650	—	−0.653

Table 6: Soil parameters for the 10-storey V-braced steel space frame on elastic foundation.

Algorithm	γ	k (kN/m^3)	$2t$ (kN/m^3)
Teaching-learning-based optimization	4.70318	11306.947	67945.018
Harmony search algorithm	4.70957	11322.086	67853.886

space frame on elastic foundation are presented in Table 4. Moreover, Figures 7 and 8 display settlements of the soil surface for two different algorithm methods and design histories of optimum solutions, respectively.

5.2. V-Braced Steel Space Frame. Figure 9 shows the typical 2D view of a V-braced steel space frame without and with soil-structure interaction. Optimum results of the V-braced space frame are shown in Table 5. Soil parameters for the space frame on elastic foundation are given in Table 6. Also, Figures 10 and 11 show the soil surface settlements obtained using two different algorithms and design histories of optimum solutions, respectively.

5.3. Z-Braced Steel Space Frame. Figure 12 represents the 2D side view of a Z-braced steel space frame without and with

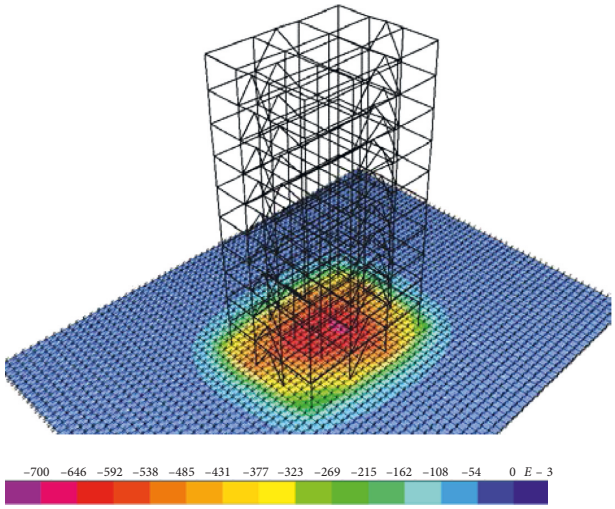

(a)

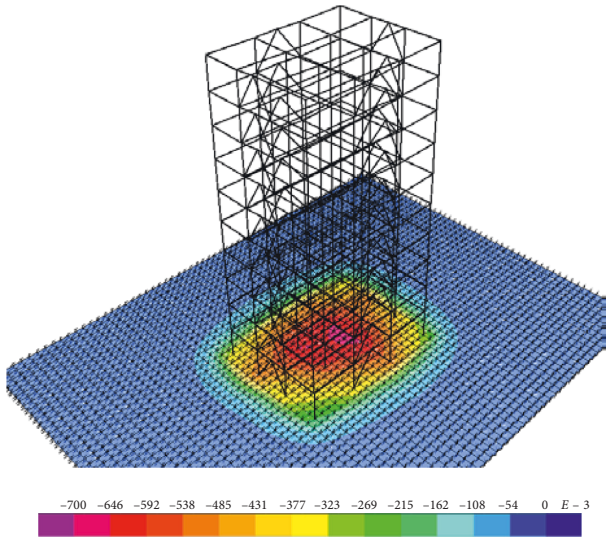

(b)

Figure 10: Settlements of soil surface for the V-braced steel space frame with two different algorithm methods (cm). (a) TLBO. (b) HS.

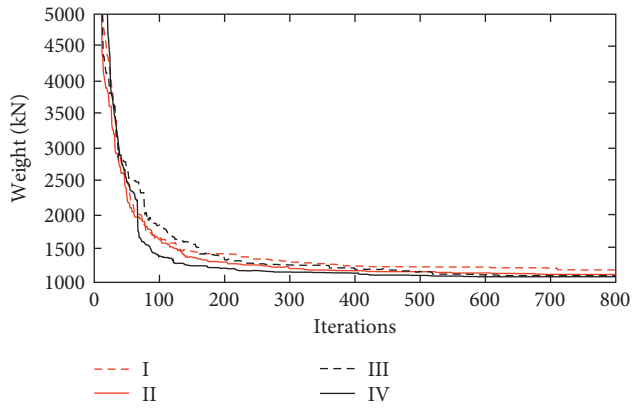

Figure 11: Design histories of the 10-storey V-braced steel space frame. I: HS with soil-structure interaction; II: HS without soil-structure interaction; III: TLBO with soil-structure interaction; IV: TLBO without soil-structure interaction.

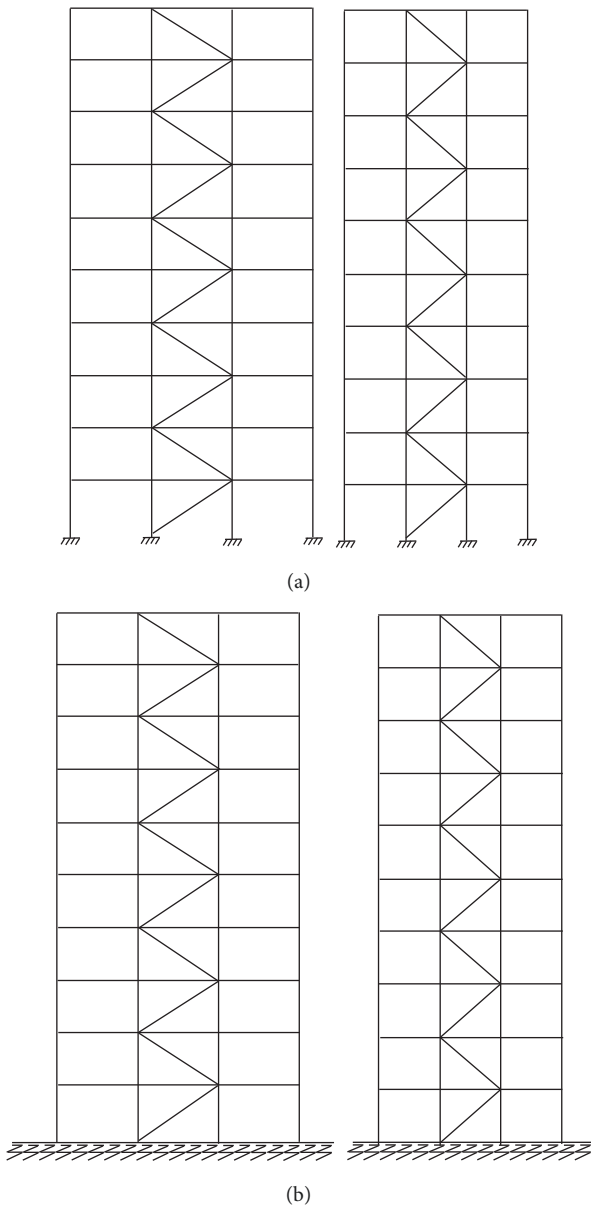

(a)

(b)

Figure 12: 2D view of the Z-braced steel space frame without and with soil-structure interaction. (a) The case without soil-structure interaction. (b) The case with soil-structure interaction.

soil-structure interaction. Optimum results of the Z-braced space frame are presented in Table 7. Soil parameters for the space frame on elastic foundation are given in Table 8. Moreover, Figures 13 and 14 represent settlements of the soil surface carried out with two different algorithm methods and design histories of optimum solutions, respectively.

5.4. Eccentric V-Braced Steel Space Frame. Figure 15 shows the 2D side view of an eccentric V-braced steel space frame without and with soil-structure interaction. The braces are connected to the beam from one-third of the beam length. Optimum results of the eccentric V-braced space frame are presented in Table 9. Soil parameters for the space frame on elastic foundation are presented in Table 10. Moreover,

Table 7: Optimum results of the Z-braced space frame.

Storeys	Member groups	Literature research, Hasancebi [36]	This study			
			TLBO without soil-structure interaction	TLBO with soil-structure interaction	HS without soil-structure interaction	HS with soil-structure interaction
1-2	CC		W8 × 31	W8 × 31	W8 × 35	W8 × 31
	OC_l		W21 × 83	W16 × 67	W12 × 65	W10 × 68
	OC_s		W24 × 103	W30 × 108	W14 × 132	W30 × 108
	IC		W12 × 106	W14 × 99	W18 × 106	W14 × 109
	OB		W8 × 24	W8 × 24	W8 × 24	W8 × 28
	IB		W10 × 33	W12 × 35	W12 × 35	W14 × 43
	BR		W6 × 15	W8 × 24	W12 × 30	W8 × 15
3-4	CC		W10 × 54	W8 × 35	W16 × 36	W14 × 30
	OC_l		W10 × 49	W14 × 90	W12 × 35	W12 × 65
	OC_s		W14 × 74	W30 × 108	W12 × 72	W18 × 55
	IC		W14 × 74	W21 × 68	W16 × 77	W21 × 73
	OB		W16 × 36	W8 × 24	W8 × 24	W8 × 24
	IB		W16 × 40	W12 × 35	W12 × 35	W14 × 38
	BR		W5 × 16	W12 × 16	W12 × 19	W8 × 24
5-6	CC		W8 × 24	W8 × 31	W8 × 35	W8 × 31
	OC_l		W8 × 31	W10 × 49	W10 × 54	W8 × 35
	OC_s		W24 × 55	W16 × 45	W16 × 50	W21 × 68
	IC		W18 × 65	W24 × 55	W18 × 60	W24 × 62
	OB		W8 × 24	W16 × 36	W12 × 30	W16 × 36
	IB		W14 × 38	W14 × 34	W12 × 35	W14 × 34
	BR		W8 × 15	W12 × 22	W6 × 15	W8 × 28
7-8	CC		W8 × 24	W8 × 24	W8 × 31	W8 × 40
	OC_l		W10 × 49	W8 × 31	W14 × 48	W12 × 35
	OC_s		W18 × 35	W14 × 43	W16 × 36	W14 × 48
	IC		W18 × 50	W16 × 40	W12 × 40	W27 × 84
	OB		W10 × 30	W8 × 24	W16 × 36	W12 × 35
	IB		W12 × 35	W14 × 34	W10 × 33	W10 × 33
	BR		W12 × 14	W10 × 15	W12 × 14	W10 × 15
9-10	CC		W8 × 31	W8 × 31	W14 × 34	W8 × 31
	OC_l		W10 × 26	W8 × 35	W10 × 33	W14 × 30
	OC_s		W12 × 26	W8 × 40	W10 × 33	W10 × 33
	IC		W14 × 43	W14 × 34	W12 × 45	W12 × 45
	OB		W10 × 26	W24 × 55	W14 × 34	W14 × 30
	IB		W10 × 33	W14 × 34	W16 × 36	W16 × 36
	BR		W12 × 14	W12 × 14	W12 × 14	W12 × 14
Weight (kN)		1058.90	1095.27	1151.40	1124.00	1166.02
Maximum lateral displacement (cm)		—	7.98	7.84	7.21	8.19
Interstorey drift (cm)		—	0.91	0.915	0.915	0.915
Maximum settlement (cm)		—	—	−0.660	—	−0.669

Table 8: Soil parameters for the 10-storey Z-braced steel space frame on elastic foundation.

Algorithm methods	γ	k (kN/m^3)	$2t$ (kN/m^3)
Teaching-learning-based optimization	4.52586	10887.654	70571.370
Harmony search algorithm	4.50073	10828.379	70959.363

Figures 16 and 17 show settlements of the soil surface carried out with two different algorithm methods and design histories of optimum solutions, respectively.

It is observed from Tables 3, 5, and 7 that the minimum weights of the braced frames for the case without soil-structure interaction are very similar to the ones available in literature research [36]. In this study, the V-braced type provides the lowest steel weight of 1083.80 kN by using teaching-learning-based optimization. Z-braced and X-braced types provide the second and third low weights, 1095.27 kN and 1170.03, respectively. Moreover, the minimum weight of the eccentric V-braced frame, 1275.01 kN, is nearly 15%, 14.1%, and 8.2% heavier than the minimum steel weights of the V-, Z-, and X-braced frames, respectively. On the other hand, harmony search algorithm presents 2.6–4.7% heavier minimum steel weights than the ones obtained from teaching-learning-based optimization for the case without soil-structure interaction. The tables including optimum results also show that the value of interstorey drift is very close to the limit value (h/400). Therefore, the displacement constraints play very crucial roles in the optimum design of the braced frames. Five

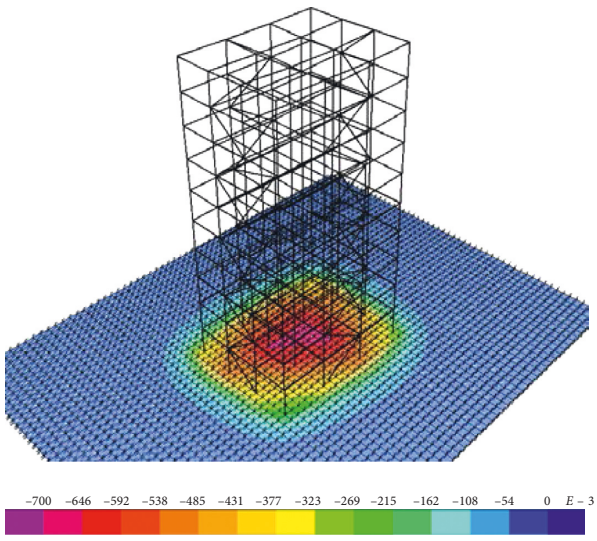

(a)

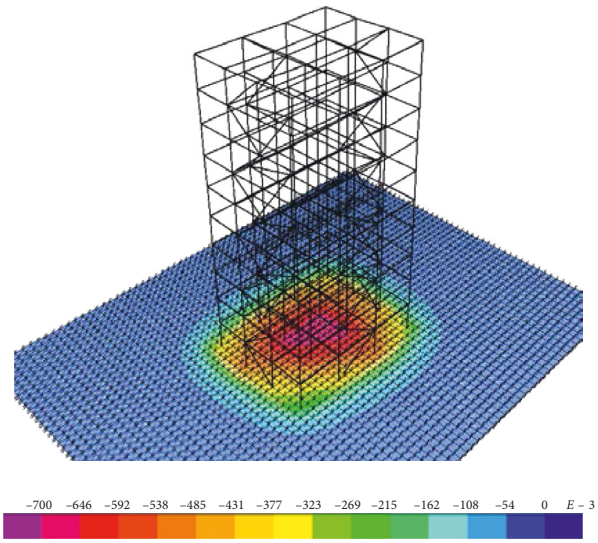

(b)

Figure 13: Settlements of soil surface for the Z-braced steel space frame with two different algorithm methods (cm). (a) TLBO. (b) HS.

independent runs are performed for each braced type for the case without soil-structure interaction.

In the case with soil-structure interaction, the minimum weights of all braced frames increased depending on settlements on the soil surfaces. It is observed from Tables 4, 6, 8, and 10 that the soil parameters of 10-storey braced steel frames on elastic foundation are similar for all cases. The minimum steel weights are mostly obtained by teaching-learning-based optimization. For the X-braced frame, the minimum weight obtained by TLBO for the case with soil-structure interaction is 4.01% heavier than the weight of the frame excluding soil-structure interaction. This ratio is 5.32% for the harmony search algorithm. Moreover, settlement values on the soil surfaces are nearly −0.66 cm as seen in Figure 7. For the V-braced frame including soil-structure interaction, TLBO and HS present 1.66 and 5.9% heavier weights, respectively. The settlements in this braced

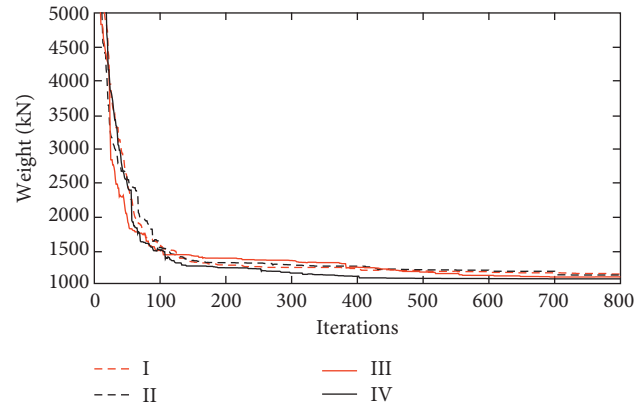

Figure 14: Design histories of the 10-storey Z-braced steel space frame. I: HS with soil-structure interaction; II: TLBO with soil-structure interaction; III: HS without soil-structure interaction; IV: TLBO without soil-structure interaction.

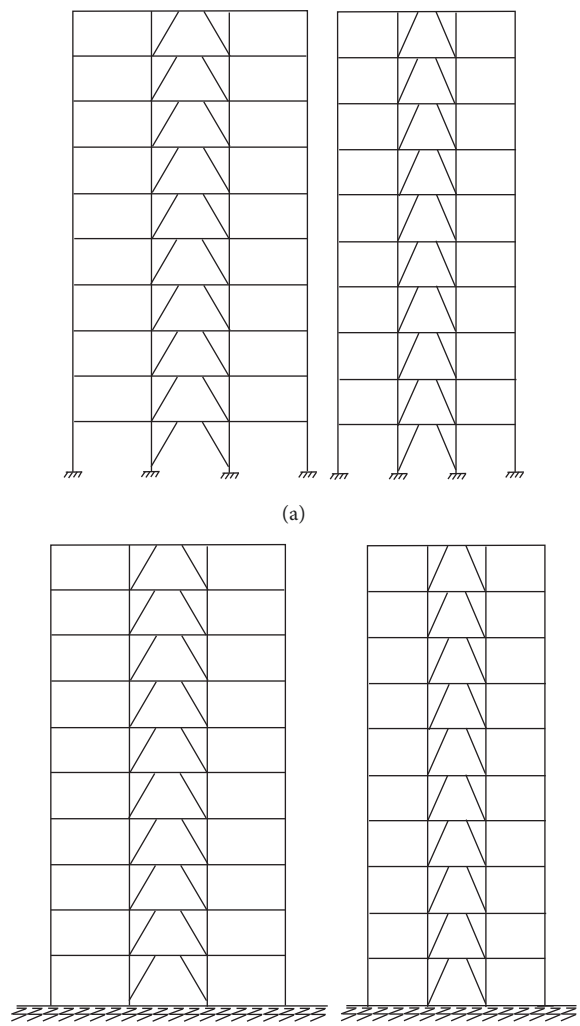

(a)

(b)

Figure 15: 2D view of the eccentric V-braced steel space frame without and with soil-structure interaction. (a) The case without soil-structure interaction. (b) The case with soil-structure interaction.

Table 9: Optimum results of the eccentric V-braced space frame.

Storeys	Member groups	This study			
		TLBO without soil-structure interaction	TLBO with soil-structure interaction	HS without soil-structure interaction	HS with soil-structure interaction
	CC	W24 × 68	W14 × 14	W14 × 14	W10 × 10
	OC_l	W24 × 24	W12 × 12	W14 × 14	W12 × 12
	OC_s	W36 × 36	W14 × 14	W10 × 10	W40 × 40
1-2	IC	W14 × 14	W10 × 10	W18 × 18	W12 × 12
	OB	W10 × 10	W18 × 18	W18 × 18	W16 × 16
	IB	W18 × 18	W16 × 16	W8 × 8	W16 × 16
	BR	W10 × 10	W16 × 16	W10 × 10	W8 × 8
	CC	W10 × 10	W12 × 12	W18 × 18	W14 × 14
	OC_l	W12 × 12	W12 × 12	W14 × 14	W12 × 12
	OC_s	W10 × 10	W12 × 12	W12 × 12	W21 × 21
3-4	IC	W27 × 27	W14 × 14	W14 × 14	W14 × 14
	OB	W18 × 18	W16 × 16	W16 × 16	W16 × 16
	IB	W12 × 12	W24 × 24	W10 × 10	W16 × 16
	BR	W12 × 12	W10 × 10	W10 × 10	W12 × 12
	CC	W12 × 12	W12 × 12	W16 × 16	W10 × 10
	OC_l	W12 × 12	W10 × 10	W12 × 12	W8 × 8
	OC_s	W24 × 24	W12 × 12	W12 × 12	W12 × 12
5-6	IC	W14 × 14	W16 × 16	W24 × 24	W24 × 24
	OB	W18 × 18	W12 × 12	W14 × 14	W16 × 16
	IB	W14 × 14	W24 × 24	W16 × 16	W14 × 14
	BR	W10 × 10	W6 × 6	W12 × 12	W6 × 6
	CC	W10 × 10	W12 × 12	W8 × 8	W14 × 14
	OC_l	W16 × 16	W8 × 8	W12 × 12	W12 × 12
	OC_s	W10 × 10	W8 × 8	W16 × 16	W14 × 14
7-8	IC	W10 × 10	W18 × 18	W10 × 10	W10 × 10
	OB	W12 × 12	W8 × 8	W16 × 16	W8 × 8
	IB	W14 × 14	W14 × 14	W10 × 10	W10 × 10
	BR	W12 × 12	W12 × 12	W12 × 12	W12 × 12
	CC	W12 × 12	W8 × 8	W14 × 14	W14 × 14
	OC_l	W8 × 8	W10 × 10	W10 × 10	W8 × 8
	OC_s	W8 × 8	W12 × 12	W10 × 10	W10 × 10
9-10	IC	W14 × 14	W10 × 10	W14 × 14	W12 × 12
	OB	W8 × 8	W8 × 8	W10 × 10	W14 × 14
	IB	W12 × 12	W10 × 10	W14 × 14	W10 × 10
	BR	W10 × 10	W12 × 12	W12 × 12	W6 × 6
Weight (kN)		1275.01	1355.05	1335.23	1441.58
Maximum lateral displacement (cm)		7.76	8.09	7.51	7.66
Interstorey drift (cm)		0.91	0.915	0.91	0.915
Maximum settlement (cm)		—	−0.609	—	−0.609

Table 10: Soil parameters for the 10-storey eccentric V-braced steel space frame on elastic foundation.

Algorithm	γ	k (kN/m^3)	$2t$ (kN/m^3)
Teaching-learning-based optimization	5.04545	12120.214	63375.683
Harmony search algorithm	5.01478	12047.186	63760.516

frame are nearly −0.65 cm as given in Figure 10. For the Z-braced frame with soil-structure interaction, the minimum weights obtained are 5.11% and 3.73% heavier by using TLBO and HS, respectively. The settlements in this braced frame are similar to the ones of the other braced frames. For the eccentric V-braced frame with soil-structure interaction, the minimum steel weights obtained are 6.27 and 7.94% heavier by using TLBO and HS, respectively. Moreover, the convergences of optimum solutions with iteration steps are seen in Figures 8, 11, 13, and 17 in detail.

6. Summary and Conclusions

In this study, the optimum design of a 10-storey steel space frame braced with X, V, Z, and eccentric V-shaped bracings including soil-structure interaction is investigated. Optimum solutions are obtained using two different metaheuristic algorithm methods: teaching-learning-based optimization (TLBO) and harmony search (HS). For this purpose, a code is developed in MATLAB computer program incorporated with SAP2000-OAPI (open application programming interface). Required cross sections are automatically selected from a list of 128 W profiles taken from AISC (American Institute of Steel Construction). The

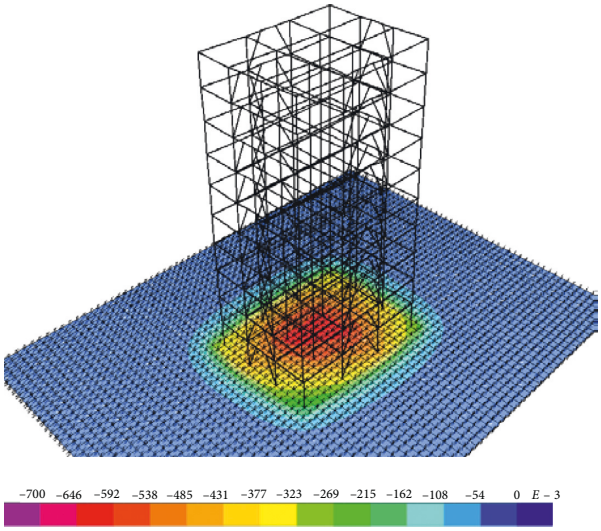

(a)

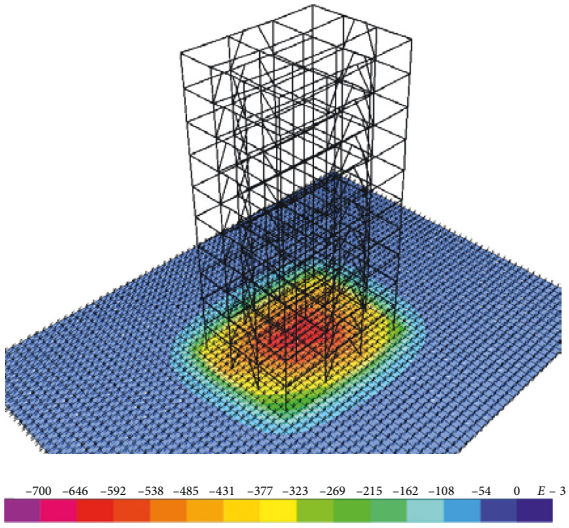

(b)

Figure 16: Settlements of soil surface for the eccentric V-braced steel space frame with two different algorithm methods (cm). (a) TLBO. (b) HS.

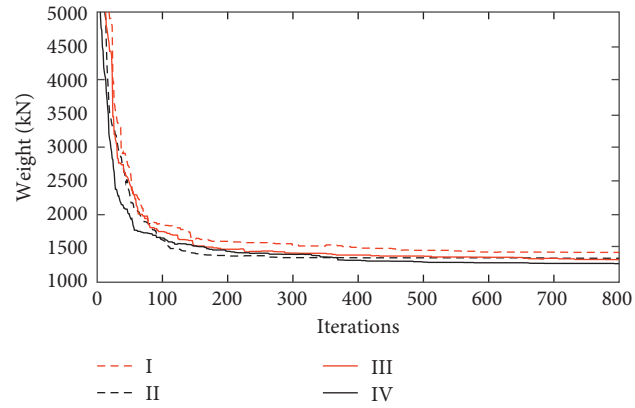

Figure 17: Design histories of the 10-storey eccentric V-braced steel space frame. I: HS with soil-structure interaction; II: TLBO with soil-structure interaction; III: HS without soil-structure interaction; IV: TLBO without soil-structure interaction.

frame model is exposed to wind loads according to ASCE7-05 in addition to dead, live, and snow loads. The stress constraints in accordance with AISC-ASD (American Institute of Steel Construction-Allowable Stress Design), maximum lateral displacement constraints, interstorey drift constraints, and beam-to-column connection constraints are applied in analyses. A three-parameter Vlasov elastic foundation model is used to consider the soil-structure interaction effect. The summary of the results obtained in this study are briefly listed below:

(i) It is observed from analyses that the minimum weight of the space frame varies by the types of bracing. The lowest steel weight, 1083.80 kN, is obtained for the V-braced steel frame by using TLBO. Z-braced and X-braced types provide the second and third low weights, 1095.27 kN and 1170.03, respectively. These results are similar to the ones available in literature [36]. The heaviest among them is the minimum weight of the eccentric V-braced frame, 1275.01 kN.

(ii) Harmony search algorithm presents 2.6–4.7% heavier steel weights than the ones obtained from teaching-learning-based optimization for the frames without soil-structure interaction. Although the lighter analysis results are obtained in TLBO, a representative structure model in TLBO is analyzed twice in an iteration step by SAP2000 programming. On the other hand, it is enough to analyze the system once in HS. This situation requires longer time for the analysis in TLBO.

(iii) Interstorey drift values are very close to its limit value of 0.915 cm (h/400). Therefore, the constraints are important determinants of the optimum design of the braced frames.

(iv) Consideration of soil-structure interaction results in heavier steel weight. For the X-braced frame including soil-structure interaction, the minimum weights are obtained to be 4.01 and 5.32% heavier by using TLBO and HS, respectively. For the V-braced frame, these values are calculated to be 1.66 and 5.9% heavier, respectively. For the Z-braced frame, these values are obtained to be 5.11% and 3.73% heavier, respectively. Moreover, for the eccentric V-braced frame, the minimum weights are obtained to be 6.27 and 7.94% heavier by these algorithm methods.

(v) Settlement values on the soil surfaces are nearly 0.61–0.67 cm for all braced frames.

(vi) Finally, the techniques used in optimizations seem to be quite suitable for practical applications. An adaptive setting for the parameters will be very useful and user-friendly especially for the structures with a large number of members as in the case here. This will be considered in future studies.

Conflicts of Interest

The authors declare that they have no conflicts of interest.

References

[1] A. Daloglu and M. Armutcu, "Optimum design of plane steel frames using genetic algorithm," *Teknik Dergi*, vol. 9, pp. 483–487, 1998.

[2] E. S. Kameshki and M. P. Saka, "Optimum design of nonlinear steel frames with semi-rigid connections using a genetic algorithm," *Computers & Structures*, vol. 79, no. 17, pp. 1593–1604, 2001.

[3] K. S. Lee and Z. W. Geem, "A new structural optimization method based on the harmony search algorithm," *Computers & Structures*, vol. 82, no. 9-10, pp. 781–798, 2004.

[4] M. S. Hayalioglu and S. O. Degertekin, "Minimum cost design of steel frames with semi-rigid connections and column bases via genetic optimization," *Computers & Structures*, vol. 83, no. 21-22, pp. 1849–1863, 2005.

[5] O. Kelesoglu and M. Ülker, "Multi-objective fuzzy optimization of space trusses by Ms-Excel," *Advances in Engineering Software*, vol. 36, no. 8, pp. 549–553, 2005.

[6] S. O. Degertekin, "A comparison of simulated annealing and genetic algorithm for optimum design of nonlinear steel space frames," *Structural and Multidisciplinary Optimization*, vol. 34, no. 4, pp. 347–359, 2007.

[7] Y. Esen and M. Ülker, "Optimization of multi storey space steel frames, materially and geometrically properties nonlinear," *Journal of the Faculty of Engineering and Architecture of Gazi University*, vol. 23, pp. 485–494, 2008.

[8] M. P. Saka, "Optimum design of steel sway frames to BS5950 using harmony search algorithm," *Journal of Constructional Steel Research*, vol. 65, no. 1, pp. 36–43, 2009.

[9] S. O. Degertekin and M. S. Hayalioglu, "Harmony search algorithm for minimum cost design of steel frames with semi-rigid connections and column bases," *Structural and Multidisciplinary Optimization*, vol. 42, no. 5, pp. 755–768, 2010.

[10] O. Hasancebi, S. Carbas, E. Dogan, F. Erdal, and M. P. Saka, "Comparison of non-deterministic search techniques in the optimum design of real size steel frames," *Computers & Structures*, vol. 88, no. 17-18, pp. 1033–1048, 2010.

[11] O. Hasançebi, S. Çarbaş, and M. P. Saka, "Improving the performance of simulated annealing in structural optimization," *Structural and Multidisciplinary Optimization*, vol. 41, no. 2, pp. 189–203, 2010.

[12] O. Hasancebi, T. Bahcecioglu, O. Kurc, and M. P. Saka, "Optimum design of high-rise steel buildings using an evolution strategy integrated parallel algorithm," *Computers & Structures*, vol. 89, no. 21-22, pp. 2037–2051, 2011.

[13] V. Togan, "Design of planar steel frames using teaching–learning based optimization," *Engineering Structures*, vol. 34, pp. 225–232, 2012.

[14] I. Aydogdu and M. P. Saka, "Ant colony optimization of irregular steel frames including elemental warping effect," *Advances in Engineering Software*, vol. 44, no. 1, pp. 150–169, 2012.

[15] T. Dede and Y. Ayvaz, "Structural optimization with teaching-learning-based optimization algorithm," *Structural Engineering and Mechanics*, vol. 47, no. 4, pp. 495–511, 2013.

[16] T. Dede, "Optimum design of grillage structures to LRFD-AISC with teaching-learning based optimization," *Structural and Multidisciplinary Optimization*, vol. 48, no. 5, pp. 955–964, 2013.

[17] O. Hasançebi, T. Teke, and O. Pekcan, "A bat-inspired algorithm for structural optimization," *Computers & Structures*, vol. 128, pp. 77–90, 2013.

[18] M. P. Saka and Z. W. Geem, "Mathematical and metaheuristic applications in design optimization of steel frame structures: an extensive review," *Mathematical Problems in Engineering*, vol. 2013, Article ID 271031, 33 pages, 2013.

[19] O. Hasançebi and S. Çarbaş, "Bat inspired algorithm for discrete size optimization of steel frames," *Advances in Engineering Software*, vol. 67, pp. 173–185, 2014.

[20] T. Dede, "Application of teaching-learning-based-optimization algorithm for the discrete optimization of truss structures," *KSCE Journal of Civil Engineering*, vol. 18, no. 6, pp. 1759–1767, 2014.

[21] S. K. Azad and O. Hasancebi, "Discrete sizing optimization of steel trusses under multiple displacement constraints and load case using guided stochastic search technique," *Structural and Multidisciplinary Optimization*, vol. 52, no. 2, pp. 383–404, 2015.

[22] M. Artar and A. T. Daloğlu, "Optimum design of composite steel frames with semi-rigid connections and column bases via genetic algorithm," *Steel and Composite Structures*, vol. 19, no. 4, pp. 1035–1053, 2015.

[23] M. Artar, "Optimum design of steel space frames under earthquake effect using harmony search," *Structural Engineering and Mechanics*, vol. 58, no. 3, pp. 597–612, 2016.

[24] M. Artar, "Optimum design of braced steel frames via teaching learning based optimization," *Steel and Composite Structures*, vol. 22, no. 4, pp. 733–744, 2016.

[25] S. Carbas, "Design optimization of steel frames using an enhanced firefly algorithm," *Engineering Optimization*, vol. 48, no. 12, pp. 2007–2025, 2016.

[26] A. T. Daloglu, M. Artar, K. Ozgan, and A. I. Karakas, "Optimum design of steel space frames including soil–structure interaction," *Structural and Multidisciplinary Optimization*, vol. 54, no. 1, pp. 117–131, 2016.

[27] M. P. Saka, O. Hasançebi, and Z. W. Geem, "Metaheuristics in structural optimization and discussions on harmony search algorithm," *Swarm and Evolutionary Computation*, vol. 28, pp. 88–97, 2016.

[28] I. Aydogdu, "Cost optimization of reinforced concrete cantilever retaining walls under seismic loading using a biogeography-based optimization algorithm with Levy flights," *Engineering Optimization*, vol. 49, no. 3, pp. 381–400, 2017.

[29] MATLAB, *The Language of Technical Computing*, The Mathworks Inc., Natick, MA, USA, 2009.

[30] SAP2000, *Integrated Finite Elements Analysis and Design of Structures*, Computers and Structures Inc., Berkeley, CA, USA, 2008.

[31] ASCE7-05, *Minimum Design Loads for Building and Other Structures*, American Society of Civil Engineering, Reston, VA, USA, 2005.

[32] AISC–ASD, *Manual of Steel Construction, Allowable Stress Design*, American Institute of Steel Construction, Chicago, IL, USA, 1989.

[33] P. Dumonteil, "Simple equations for effective length factors," *Engineering Journal. AISC*, vol. 29, pp. 111–115, 1992.

[34] C. V. G. Vallabhan and A. T. Daloglu, "Consistent FEM-Vlasov model for plates on layered soil," *Journal of Structural Engineering*, vol. 125, no. 1, pp. 108–113, 1999.

[35] R. V. Rao, V. J. Savsani, and D. P. Vakharia, "Teaching-learning-based optimization: a novel method for constrained mechanical design optimization problems," *Computer-Aided Design*, vol. 43, no. 3, pp. 303–315, 2011.

[36] O. Hasancebi, "Cost efficiency analyses of steel frameworks for economical design of multi-storey buildings," *Journal of Constructional Steel Research*, vol. 128, pp. 380–396, 2017.